

Accepted Manuscript

Investigation of the Fouling Effect on a Commercial Semi-Permeable Membrane in the Pressure Retarded Osmosis (PRO) Process

Elham Abbasi-Garravand, Catherine N. Mulligan, Claude B. Laflamme, Guillaume Clairet

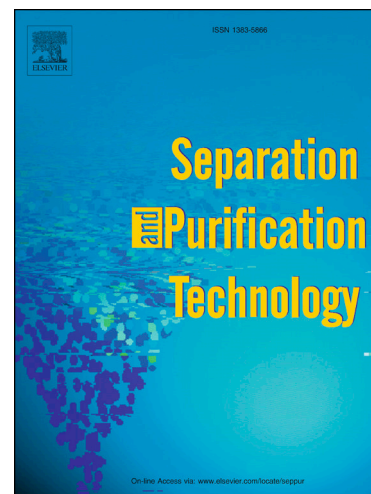
PII: S1383-5866(17)31428-4
DOI: <https://doi.org/10.1016/j.seppur.2017.10.053>
Reference: SEPPUR 14135

To appear in: *Separation and Purification Technology*

Received Date: 4 May 2017
Revised Date: 26 October 2017
Accepted Date: 26 October 2017

Please cite this article as: E. Abbasi-Garravand, C.N. Mulligan, C.B. Laflamme, G. Clairet, Investigation of the Fouling Effect on a Commercial Semi-Permeable Membrane in the Pressure Retarded Osmosis (PRO) Process, *Separation and Purification Technology* (2017), doi: <https://doi.org/10.1016/j.seppur.2017.10.053>

This is a PDF file of an unedited manuscript that has been accepted for publication. As a service to our customers we are providing this early version of the manuscript. The manuscript will undergo copyediting, typesetting, and review of the resulting proof before it is published in its final form. Please note that during the production process errors may be discovered which could affect the content, and all legal disclaimers that apply to the journal pertain.



Investigation of the Fouling Effect on a Commercial Semi-Permeable Membrane in the Pressure Retarded Osmosis (PRO) Process

Elham Abbasi-Garravand¹, Catherine N. Mulligan^{1*}, Claude B. Laflamme²,
Guillaume Clairet³

1-Department of Building, Civil and Environmental Engineering, Concordia University, 1455 de Maisonneuve Blvd. W., Montreal, Quebec, Canada H3G1M8

*2-Institut de recherche d'Hydro-Québec, Shawinigan, Québec, Canada
3-H2O Innovation Inc., Québec City, Québec, Canada*

**Corresponding author; Tel: +1(514) 848-2424, ext 7925, Fax: +1(514)848-7965, email:*

catherine.mulligan@concordia.ca

ABSTRACT

One of the main challenges for generating osmotic power by using PRO technology is the membrane fouling which reduces the permeate flux and consequently increases the cost and decreases the osmotic power generation. In this research, different feed waters with various qualities were used to investigate the effect of fouling on a commercial membrane in PRO mode in continuous conditions. Also, the fouling mechanisms were investigated in order to study the cleaning of the membrane in PRO mode in the future research. In addition, four classic fouling models such as complete blocking model (CBM), intermediate blocking model (IBM), standard blocking model (SBM) and cake filtration model (CFM) were used. Cake enhanced osmotic pressure as a new mechanism for osmotically driven membranes was studied as well. According to the results, the fouling rate when the draw solution was synthetic salt water followed the order of: untreated river water > multimedia sand filter > microfiltration > ultrafiltration effluents. The fouling rate in ultrafiltration and microfiltration effluents using sea water occurred faster compared to the results for untreated synthetic salt water. Complete fouling (permeate flux was negligible)

occurred after 580 hours using feed water from ultrafiltration unit. It was observed that cake filtration and cake enhanced osmotic pressure were the main fouling mechanisms that governed the membrane fouling. These models could describe the membrane fouling in PRO processes.

Keywords: Osmotic Power, PRO Membrane, Fouling Mechanisms, Membrane Fouling

1 Introduction

The PRO technology, invented by Prof. Sidney Leob, has attracted significant attention in recent years [1-9]. Pressure Retarded Osmosis (PRO) is a technology that is used to generate osmotic power- based on salinity gradients [10]. In this membrane based technology, water moves from a feed solution with a low osmotic pressure toward a draw solution with a high osmotic pressure versus a hydraulic pressure [11]. In comparison with forward osmosis (FO) process, a back pressure is applied on the high salinity draw solution side to pressurize it and produce electricity in the PRO process. Then the power is produced by releasing the pressure from the solution through a turbine [12]. The RO process uses mechanical energy to overcome the sea water osmotic pressure, while in the PRO process, mechanical energy is produced from the chemical potential or osmotic energy of a draw solution [1].

Like other technologies, the PRO process has some disadvantages such as fouling, internal and external concentration polarization, salt reflux and high operating pressures [7]. The semi permeable membrane as the heart of the PRO process plays an important role in the osmotic power generation [8]. One of the main obstacles for using PRO technology is the membrane fouling that is a time-

dependent and ultimately an irreversible phenomenon and imposes a high cost to the system in terms of energy consumption. In the FO process, membrane fouling on the feed side is less and can be controlled simply by using hydrodynamic cleaning. However, in the PRO process, due to the deposition of the organic and inorganic species in the feed water inside the porous support layer, the efficiency of the PRO membrane reduces critically [9]. It is important to investigate and identify the fouling mechanisms to find a better cleaning method and also reduce the frequency of the fouling and consequently improve the performance of the PRO processes.

Numerous studies have been done to investigate the fouling mechanisms in membrane processes [13-19]. Hermans and Bredée [20] proposed four well-known and extensively used fouling models (cake fouling, adsorption or intermediate blocking, complete blocking and intermediate blocking) for investigation of the membrane fouling mechanisms [21-25]. In complete blocking, particles block the pores and hinder flow. In intermediate or adsorption blocking, part of the particles block the pores and the remainder are gathered on top of other deposited particles. In cake filtration, particles accumulate on the surface of the membrane and create a penetrable cake that decreases the flow. In standard blocking, particles gather inside the membrane pores. Over time, the pores become smaller due to the deposition of the particles and consequently, flow decreases [25]. In addition, it has been recently investigated that reverse flux of solutes from the draw solution into the feed solution can increase and enhance the membrane fouling in FO and PRO processes [11, 26-29].

Although much research has been done on PRO, the membrane fouling and its mechanisms have not been studied very well yet. In the few existing fouling studies on PRO membrane, artificial foulants and synthetic draw and feed solutions were

mostly used [2, 8, 11, 30]. In this research, however, river water and sea water were used as the feed and draw waters respectively to observe the effect of fouling on a commercial semi permeable membrane in PRO mode in realistic conditions. An experimental setup was used in which avoids recirculation. In this way effects such as dilution and accumulation of draw solutes in the feed are avoided. This is rarely seen in studies like this. Also various parameters were determined in raw sea water to examine the sea water characteristics. In addition, four classic fouling models such as complete blocking model (CBM), intermediate blocking model (IBM), standard blocking model (SBM) and cake filtration model (CFM) were used. The fouling models used in the study were based on cross flow configuration [31]. There is some criticism of the blocking models and their applicability to crossflow filtration. However, many researchers ([23, 32-37]) have used these classic models for prediction of fouling mechanisms in crossflow filtrations and according to their publications and results, these models were applicable to crossflow filtration. Cake enhanced osmotic pressure as a new mechanism for osmotically driven membranes was studied as well. These models were used to study the fouling mechanisms in PRO processes under real conditions.

2 Materials and Methods

2.1 Chemicals

The prepared synthetic salt water was a combination of demineralized water, sodium chloride and calcium chloride. Calcium chloride was added in order to observe the effect of calcium ion on PRO membrane fouling. The used Na/Ca ratio was selected based on its ratio in sea water [38, 39]. The mass ratio of Na/Ca was 26. As the typical salinity of Saint Lawrence River at its estuary is 30 g/L [40], the used salt

concentration was 30 g/L. Sodium chloride (NaCl-10 kg- S271-10) was used to prepare salt water in this study. This reagent salt was provided by Fisher Scientific Co. Calcium chloride dihydrate ($CaCl_2$ -3 kg-C79-3) was purchased from Fisher Scientific Co. as an additive to salt water. All experiments were done at the LTE (Laboratoire des technologies de l'énergie) in the Hydro-Québec Research Institute located at Shawinigan, Québec, Canada.

2.2 Sea Water and River Water Sampling

In all experiments, the sea water was taken from the Saint Lawrence River at the Station Aquicole located in Rimouski, Québec in the estuary of Saint Lawrence and was sent to Hydro-Québec lab at Shawinigan, Québec. Fresh water was taken from the Saint-Maurice River at the entrance of pressure channels in the hydroelectric Shawinigan-2 power plant. The river water was transported to Hydro-Québec LTE lab (Laboratoire des technologies de l'énergie) by a 2 m^3 polypropylene tank which was mounted on a trailer (Magnum Water Trailer – MWT500).

2.3 Water Quality

In order to investigate the sea water and fresh waters (river water, filtered and permeate waters from the multimedia sand filter, ultrafiltration and microfiltration) characteristics, the parameters such as color, iron, total organic carbon (TOC), silica, suspended solids, alkalinity, hardness, pH, salinity, conductivity, turbidity, dissolved solids, sodium, calcium, magnesium, potassium and silt density index (SDI) were measured. The parameters such as SDI, turbidity, hardness, monovalent and divalent cations, silica and total organic carbon (TOC) are important in membrane fouling. As the river water was brought to the lab in volumes of 2 m^3 every 2 weeks and the fouling tests were done continuously, it was not possible to use the same feed water for all experiments. The results in Tables 3 and 4

demonstrate the average physiochemical characteristics of different used feed waters and sea water.

SDI was specified by using the standard method D4189 of American Society for Testing and Measuring (ASTM). Due to the different shapes, sizes and nature of the particulates, the quality of particulates may not be measured absolutely [41]. In this method the rate of clogging ($SDI_{15}(500 \text{ mL})$) was calculated by passing a fixed volume of the water (500 mL) through a 0.45 μm membrane filter during a specific time (15 min) at a constant pressure of 30 Psi (207 kPa) [42]. The direct method (Method 10129) for the low range test (0.3 to 20 mg/L C) and the USEPA ManVer Buret titration method (Method 8226) for the range of 0 to 25000 mg/L as CaCO_3 were used for TOC and hardness respectively [43]. For color, and the iron platinum-cobalt standard method (method 8025), the USEPA FerroVer method (method 8008: 0.02 to 3 mg/L), and the 1-(2-Pyridylazo)-2- Naphthol PAN Method (method 8149) were used, respectively. The used methods for silica, and suspended solids were as follows respectively: the silicomolybdate method (method 8185: 1.0 to 100 mg/L), and the photometric method (method 8006: 5.0 to 750 mg/L). Some of these parameters such as iron, TOC, silica, sodium, potassium, calcium, and magnesium were measured at CNETE (Centre National en Électrochimie et en Technologies Environnementales located at Shawinigan, Quebec, Canada) and the rest were measured at the Hydro-Québec Research Institute.

The amount of iron, silica, sodium, potassium, calcium, and magnesium were measured by optima 4300 DV ICP-OES (Inductively Coupled Plasma Optical Emission Spectrometer) from Perkin Elmer Inc. For TOC analysis, TOC-L (Laboratory Total Organic Carbon Analyzer) from Shimadzu Corporation was used. The amount of color, and suspended solids were measured by a DR 6000™ UV VIS

Spectrophotometer from the Hach Company. Alkalinity and hardness were measured by titration of sulfuric acid (0.02 N) and titration of Titraver EDTA (0.02 N) respectively. Salinity, pH, conductivity, and dissolved solids were measured by an HQ440d Benchtop Dual Input Multi-Parameter Meter from the Hach Company. Turbidity was measured by a Ratio Turbidimeter/XR 115/230 V from the Hach Company. SDI was measured by using a Simple SDI: auto manufactured by SDI Solutions, a division of Procam Controls Inc.

2.4 Experimental Design

2.4.1 Multimedia Sand Filter System

The experimental setup for the sand filter was installed at Hydro-Québec Research Institute. Materials and equipment that were used in the multimedia sand filter bench system are the same as previous work [44]. The effluent was used for the fouling tests.

2.4.2 Ultrafiltration System

The experimental setup for a dead end ultrafiltration system was installed at the Hydro-Québec Research Institute. Materials and equipment that were used in the ultrafiltration bench system are the same as previous work [44]. The used membrane had an outside/in hollow fiber configuration with a molecular weight cut off (MWCO) of 400 kDa [45]. The used ultrafiltration membrane was selected based on the good removal results that have been achieved by Ødegaard et al. in their previous work [46-48]. The permeate was used for the fouling tests.

2.4.3 Microfiltration System

The experimental setup for microfiltration system was installed at LTE Hydro-Québec. Materials and equipment that were used in the microfiltration bench system are demonstrated in the previous work [49]. The used membrane was a double open

end glass fiber filter cartridge with a pore size of 3 microns and filtration area of 0.4 m^2 . The permeate was used for the fouling tests.

2.4.4 PRO Unit

2.4.4.1 Membrane and Spacer

The used PRO membrane was a thin-film composite (TFC) membrane with hydrophilic support layer provided by Porifera Inc. [50]. The active surface area of the membrane was 0.00875 m^2 . Table 1 indicates some specific parameters of the used TFC membrane. The membrane was soaked in deionized water for 15-20 minutes before each PRO experiment [51]. Then the wet membrane was rinsed by deionized water and was placed in the osmotic cell. The skin was faced toward the salt side [8]. In the last step, the osmotic cell was connected to the bench system while it was housed in a water bath at constant temperature. Two spacers, one on the fresh side and the other one on the salt side, were used and placed in the osmotic cell for all PRO tests. The spacers were provided by Filmtec Company. The spacers had a diamond-type mesh with thickness of 0.9 mm (filament spacing 3 mm).

Table 1: PRO Membrane Parameters [50].

Parameter	Unit	Value
Water Permeation (PRO mode)	LMH	58 ± 3
Reverse Salt Flux (RSF)	g/L	0.25 ± 0.1
Salt Rejection	%	99.6 ± 0.15
Membrane Structural Parameter	Microns	215 ± 30
Maximum Operating Temperature	°C	70
Maximum Transmembrane Pressure	kPa	1241
pH Operating Range	-	2-11
Maximum Chlorine	ppm	< 0.1

2.4.4.2 PRO Experiments

Figure 1 demonstrates the PRO membrane setup at Hydro-Québec and Table 2 shows the materials and equipment that were used on PRO membrane bench

system. As Figure 1 part b indicates salt and fresh water were pumped from salt and fresh water reservoirs to the osmotic cell which was placed in a water bath including a temperature probe, then the permeate water was passed through the PRO membrane from the fresh side to the salt side. The osmotic cell dimensions were indicated in Figure 2. The input and output flow rates of the feed water on the fresh side were measured continuously using two Bronkhorst flow meters (Table 2) connected to a computer with a logging interval of one minute or 60 seconds during the PRO experiments in the lab. The difference between these input and output flow rates was measured as the permeate flowrate. Permeate flux was calculated using Equation (1)

$$Flux \left(L/m^2.h \right) = \left[\frac{Permeate \text{ Flow rate } (mL/min)}{Cartridge \text{ Area } (m^2)} \right] \times 0.06 \quad (1)$$

Table 2: Materials and equipment in PRO membrane bench system [52].

Material	Quantity	Supplier	Code	Capacity
Pumps				
Salt and Fresh Water Pumps	2	Cole Parmer	EW-07128-10	31 mL/min
Detergents Pump	1	Cole Parmer	EW-07128-25	390 mL/min
Reservoirs				
Reservoirs	2	Ace	AC-SP0003RT	10 L
Sensors				
Manometer	1	Swagelok	PGI-63B-PG30-LAQX	0-30 psi (0-206.84 kPa)
Pressure Gauge	1	Cole Parmer	68403-00	0-30 psi (0-206.84 kPa)
Flow meter	3	Bronkhorst	Liqui-flow #L23-ABG-22-K	0-10 mL/min
Temperature Probe	1	Omega	PR-24-3-100-A-1/4-1/4-6	RTD
Osmotic Cell				
Osmotic Cell	1	Local Fabrication	-	87.5 cm ² of surface active
Water Bath	1	Cole Parmer	PD07R-20	-20 to 150 °C ± 0,005 °C reservoir of 7 litres

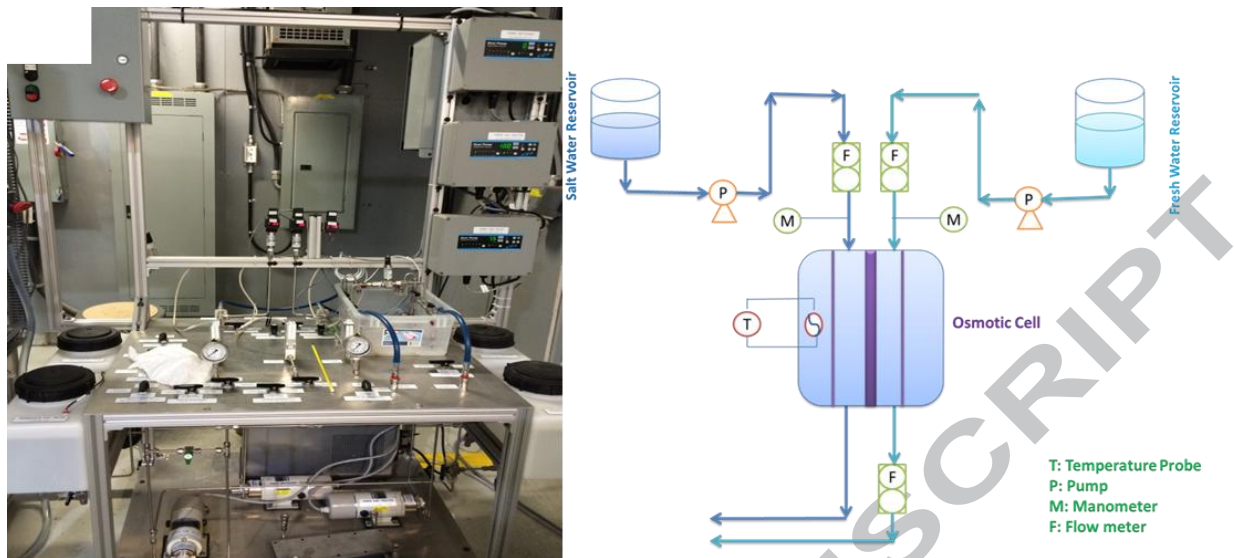


Figure 1: a) PRO Membrane setup at Hydro-Québec Research Institute, b) A schematic of PRO membrane setup.

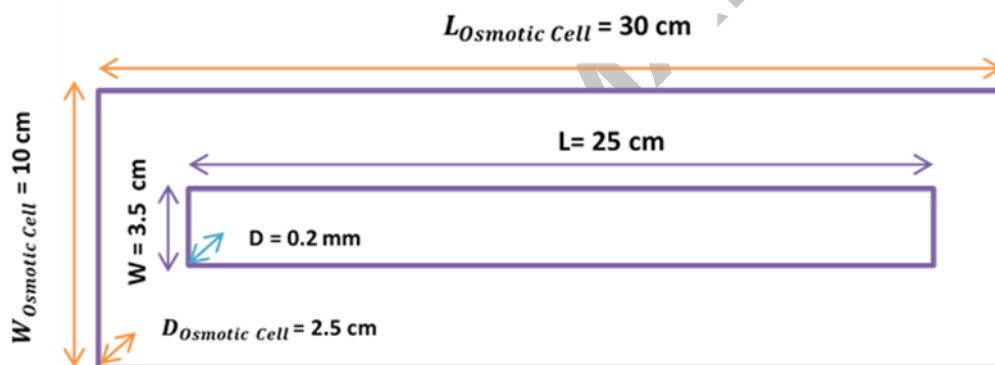


Figure 2: Osmotic Cell Dimensions.

All experiments were performed at Hydro-Québec LTE. Cross flow velocities of 5 cm/s and 4.84 cm/s were applied on the salt and fresh sides, respectively. In recent PRO research, hydraulic pressure was applied on the salt side in a range of 0.48 to 15.4 bar (48 to 1540 kPa) [2-4, 11, 53-60]. In this research the applied hydraulic pressure on the salt side was 3 bar (300 kPa) due to the device limitation. The initial conditions such as pressure, temperature, synthetic salt concentration, and sea water salt concentration were constant for all fouling experiments and were 300 kPa (3 bars), 25°C, 30 g/L respectively. Four different feed waters including untreated

water (river water), permeate water from ultrafiltration system, filtered water from multimedia sand filter, and permeate water from microfiltration system were used to perform the fouling tests. In this research for simplification, these four feed waters were mentioned as untreated water, ultrafiltration, multimedia sand filter, and microfiltration waters respectively. The two different draw solutions were synthetic salt water and sea water. As the salinity of the four feed waters was zero (Table 3), the osmosis pressure of the four feed water solutions was assumed to be zero.

2.5 Fouling Models

Four classic fouling models such as CBM, IBM, SBM and CFM were used to investigate the fouling behavior of the membrane in PRO mode. In all fouling tests, the decline of permeate flux over time at constant pressure was studied. The equations for permeate flow rate at constant pressure are summarized in Table 5. As using linearized forms are more suitable for data analysis and model identification [23], [31], the linearized forms of these models were used in this research. The regression squared (R^2) was used as an index to investigate the agreement of the experimental data with the used model. This means that when the R^2 is equal to one, the experimental data is completely in agreement with the used model.

3 Results and Discussion

3.1 PRO Membrane Fouling

3.1.1 Effect of different feed solutions

As it was mentioned in section 2.4.4.2, all fouling tests were done at constant temperature, salinity and pressure. All fouling tests were continued until complete fouling was reached (permeate flux was negligible). The used draw solution was

synthetic salt water for all four feed waters (untreated river water), ultrafiltration, microfiltration, multimedia sand filter effluents). The flow rates on both feed and draw sides were 10 mL/min for all the experiments. All experiments were done in duplicate. PRO experimental setup was an open system which means the draw solution was not recirculated in the system and was continuously discharged into a waste disposal system that was in Hydro-Quebec lab, so the draw solution could not be diluted and as a result, the salt concentration remained constant during the experiments. Therefore dilution did not have any effects on the fouling and the flux drop in the experiments. In addition, according to the result reported by Tang et al. [61], internal concentration polarization (ICP) decreases when: the active layer faces the draw solution, flow rates on feed and draw sides are low, the salt concentration is low, and the salt concentration on draw side is constant. Due to the use of low flowrates on both sides of the membrane, the active layer facing the draw solution, low salt concentration on the draw solution, and constant salt concentration on the draw side (because of using an open system), the effect of internal concentration polarization was assumed negligible. According to the indicated results in Table 3, ultrafiltration had the best quality compared to microfiltration, multimedia sand filter and untreated water. The order based on their qualities was as follows: ultrafiltration > microfiltration > multimedia sand filter > untreated water (river water).

Table 3: Physio-chemical Characteristic of Ultrafiltration, Microfiltration, Multimedia Sand Filter, and River Water.

Parameters	Ultrafiltration	Microfiltration	Multimedia Sand Filter	River Water
SDI ₁₅ (500ml)	1.98	12.50	15.64	19.17
Apparent Color (mg/L PtCo)	11.57	63.00	68.47	98.00
Total Iron (mg/L Fe)	0.01	0.15	0.17	0.27
TOC (mg/LC)	3.49	6.03	6.72	7.17
Silica (mg/LSiO ₂)	2.10	2.12	2.15	2.29
Suspended Solids (mg/L)	0.14	1.00	1.00	2.00
Total Alkalinity	4.57	5.00	5.00	5.00
Hardness (mg/L as CaCO ₃)	3.67	5.00	5.00	5.00
pH	7.14	7.39	7.49	7.64
Salinity (%)	0.01	0.01	0.01	0.01
Conductivity (μS/cm)	17.27	21.40	23.90	24.00
Turbidity (NTU)	0.01	0.63	0.72	1.37
Dissolved Solids (mg/L)	8.02	9.97	11.1	11.20
Sodium (mg/L)	1.26	1.40	1.50	1.51
Calcium (mg/L)	1.37	2.19	2.23	2.28
Magnesium (mg/L)	0.39	0.58	0.59	0.61
Potassium (mg/L)	0.29	0.34	0.36	0.41

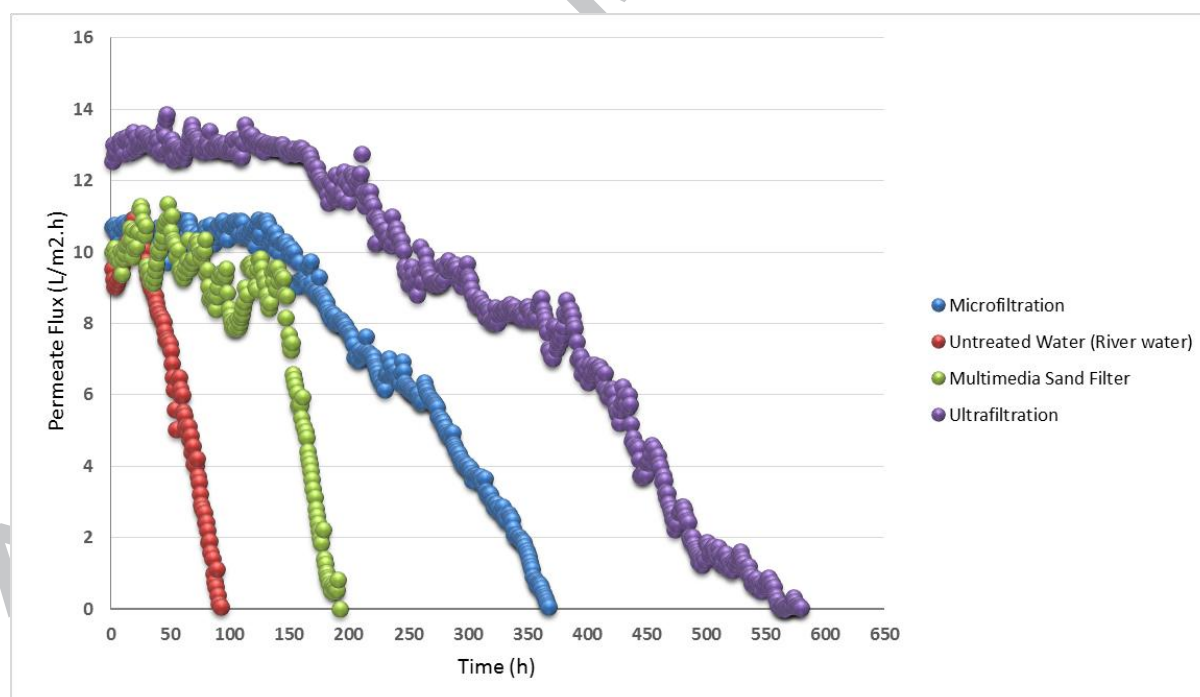


Figure 3: Effect of Fouling on Permeate Flux using Different Feed Waters

As Figure 3 shows, complete fouling occurred faster when the used feed water was river water which is in the agreement with the results in Table 3. Complete fouling occurred in ultrafiltration, microfiltration, multimedia sand filter effluents and untreated river water after passing 580, 368, 192, and 92 hours respectively. Based on the results in Figure 3, the fouling/flux decline seems to occur in two stages, a slow one, followed by a phase with a comparatively rapid flux decline. The permeate flux in the fouling tests was reduced very slowly at the beginning (it was almost constant). However, after a certain time, it started to decline dramatically with a higher rate until it reached zero. Lee et al. [26] also observed the same behavior regarding the changes of the permeate flux over time (permeate flux was nearly constant). Chen et al. [62] also reported that permeate flux was stable for 60 h using a TFC hollow fiber membrane in PRO mode. The similar findings were published by Kim et al. [63] for permeate flux during 10 h of PRO fouling experiment as well. In addition, Kim et al. [64] reported a slight decrease in permeate flux from the start point to 16 h followed by a sudden decline of 16% from 16 h to 24 h.

The smoothness of the permeate flux at the beginning might have occurred due to two reasons. The first reason can be related to the type of driving force in the PRO membrane processes which is the difference of osmotic pressure between feed and draw solutions. This means no hydraulic pressure is applied on the feed side and as a result, it does not even accelerate the fouling but, assists in delaying it. The second one is related to the quality of the feed water. As a matter of fact, the better the quality of the water, the lower the amount of particles and colloids in the water. Therefore, the aggregation of particles will be time consuming and consequently, the fouling occurs gradually. As Figure 3 demonstrates, the results are in agreement with the second reason. Wherever the quality of the feed water was better, it took more

time to reach the point when the fouling rate increased. It should be mentioned that the co-presence of silica and organic matter in feed waters (Table 3) might end up with the formation and deposition of the silica-organic matter compounds on the membrane surface and as a result increases the fouling rate rapidly [65].

3.1.2 Effect of sea water

The experiment to determine the effect of sea water was performed at constant pressure and temperature (300 kPa and 25°C). Based on the results in the previous section, ultrafiltration and microfiltration treatments indicated better results compared to no treatment and multimedia sand filter treatment. Therefore, these two feed waters were selected to perform the fouling tests with the sea water. According to the results demonstrated in Figures 4 and 5, the fouling occurred faster and earlier when the draw solution was sea water. Complete fouling occurred in ultrafiltration and microfiltration effluents after passing 405, and 230 hours, respectively. This indicates that the fouling using ultrafiltration and microfiltration effluents with sea water occurred 30% and 38% faster compared to the results for synthetic salt water. The complete fouling was chosen as an evaluation point because it shows how fast/slow the fouling occurs.

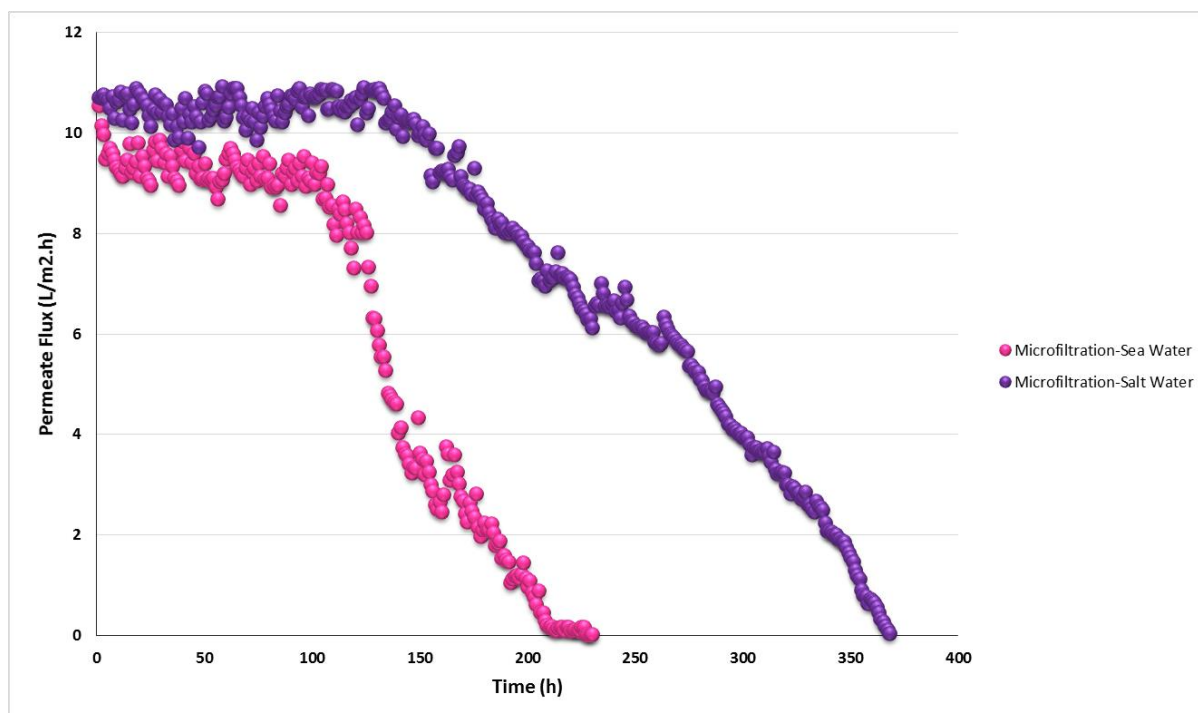


Figure 4: Effect of Fouling on Permeate Flux Using Microfiltration as Feed Water and Sea Water and Synthetic Salt Water as Draw water.

In addition, when the used draw solution was sea water and feed water was from microfiltration, the permeate flux decreased about 71.3% after one week (168 hours). However, the decline in the permeate flux for the synthetic salt water, when the used feed water was from microfiltration, was 9.2% at the same time. For ultrafiltration effluent as the feed water, the decreases in the permeate fluxes were 25.4% and 3.1% simultaneously (168 hours) for both sea water and synthetic salt water respectively. The reason can be related to the quality of sea water.

According to the results demonstrated in Table 3, the quality of microfiltration water was lower than that in the ultrafiltration water and that is why the microfiltration water seems to be more strongly affected by the sea water compared to the ultrafiltration water.

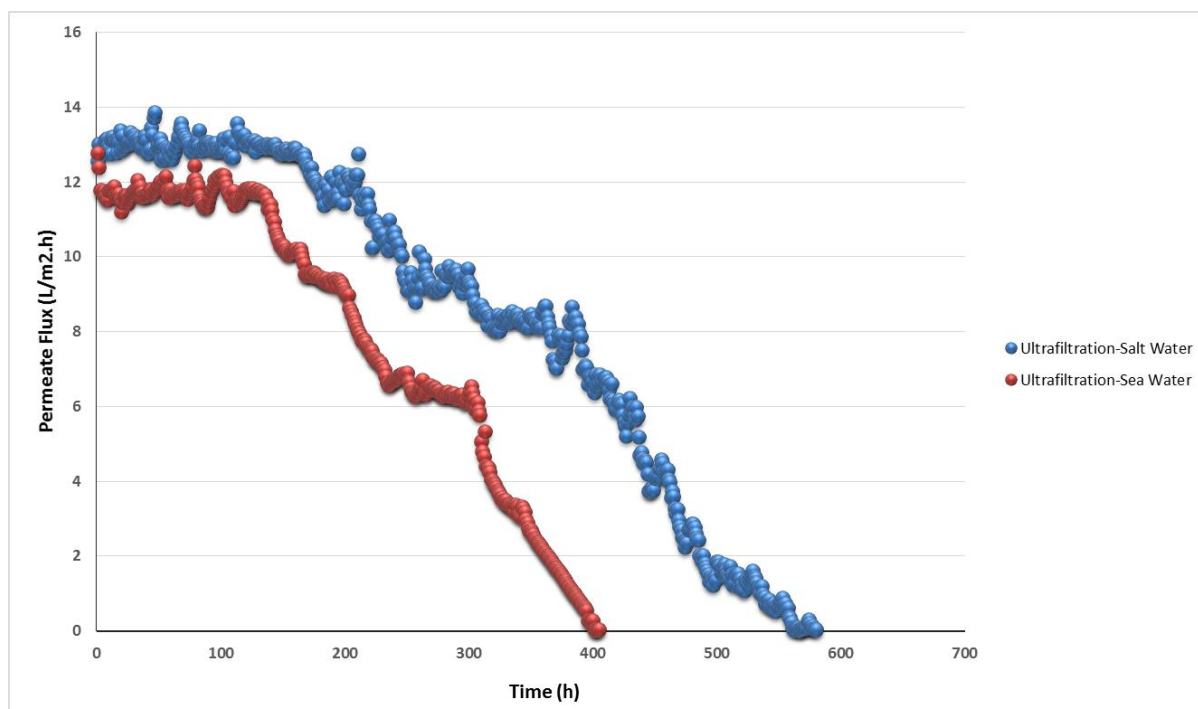


Figure 5: Effect of Fouling on Permeate Flux Using Ultrafiltration as Feed Water and Sea Water and Synthetic Salt Water as Draw water.

As the quality of ultrafiltration and microfiltration effluents were the same for both sea water and synthetic salt water, it seems that the quality of sea water played an important role on the membrane fouling in the PRO process. Because the synthetic salt water contained only sodium chloride, calcium chloride and demineralized water while the other components including higher concentration of divalent cations (Ca^{+2} and Mg^{+2}) were observed in the sea water (Table 4) that can influence the fouling rate. Identification of the type of foulants at the membrane surface and within the porous substrate and investigation of the cleaning methods for PRO processes was discussed in the previous work [49].

Table 4: Physio-chemical Characteristic of Sea Water.

Parameters	Sea Water
Apparent Color (mg/L PtCo)	7.00
Total Iron (mg/L Fe)	0.00
TOC (mg/L C)	1.85
Silica (mg/L SiO ₂)	0.7
Suspended Solids (mg/L)	0.00
Total Alkalinity	78.00
Hardness (mg/L as CaCO ₃)	4500.00
pH	7.75
Salinity (%)	30
Conductivity (μ S/cm)	37000.0
Turbidity (NTU)	0.503
Dissolved Solids (mg/L)	22.6
Sodium (mg/L)	8750.00
Calcium (mg/L)	324.00
Magnesium (mg/L)	1100.00
Potassium (mg/L)	404.00

3.2 Fouling Mechanisms

In CFM as the most frequently used model, it is assumed that the particles lay down on the membrane surface as a porous layer. The thickness of this layer increases over time and subsequently it decreases the permeate flux [23-25, 66]. As all fouling experiments were done at constant pressure (3 bars or 300 kPa), four classic fouling models at constant pressure were used (Table 5) [20, 22-24]. In order to simplify data processing, the linearized forms of these models were used for analyzing the experimental data [23]. The difference of squared regression (R^2) was used as an index to investigate the agreement of the experimental data with the used model. The equations for permeate flow rate in two forms (linearized and non-linearized) are presented in Table 5. It should be noted that a , b and β parameters mentioned in Table 5 are constant.

Table 5: Four Constant Pressure Fouling Models [23].

Fouling Mechanisms	Flux Equations	Linearized Forms
Complete Blocking (CBM)	$\frac{Q}{Q_0} = \exp(-\beta t)$	$\ln Q = at + b$
Intermediate Blocking (IBM)	$\frac{Q}{Q_0} = (1 + \beta t)^{-1}$	$\frac{1}{Q} = at + b$
Standard Blocking (SBM)	$\frac{Q}{Q_0} = (1 + \beta t)^{-2}$	$\frac{t}{V} = at + b$
Cake Filtration (CFM)	$\frac{Q}{Q_0} = (1 + \beta t)^{-0.5}$	$\frac{t}{V} = aV + b$

The CFM (Table 5) was applied to the obtained experimental data in section 3.1 in order to determine if the CFM was in agreement with the experimental data. The experimental data were selected from the beginning until the flux was reduced by 95%. According to the results demonstrated in Figures 6 and 7, the experimental data are highly in accordance with CFM. This means that over time, particles accumulated and were deposited on the membrane surface and created an incompressible cake layer (as no hydraulic pressure was applied) which reduced the permeate flux due to the hydraulic resistance. This phenomena occurred slowly at the beginning and that was why the permeate flux decreased very slowly from the start point. Over time, depending on the quality of the feed water, the cake layer thickness started growing on the membrane surface until it changed the incompressible cake layer to a denser cake layer. At this point, it seems that the sharp decrease in permeate flux occurred. The R^2 values of the four different feed waters were higher for the cake filtration model compared to the other models. The maximum and minimum values of R-squared were 0.95 and 0.84 for river water-synthetic salt water and ultrafiltration-synthetic salt water respectively.

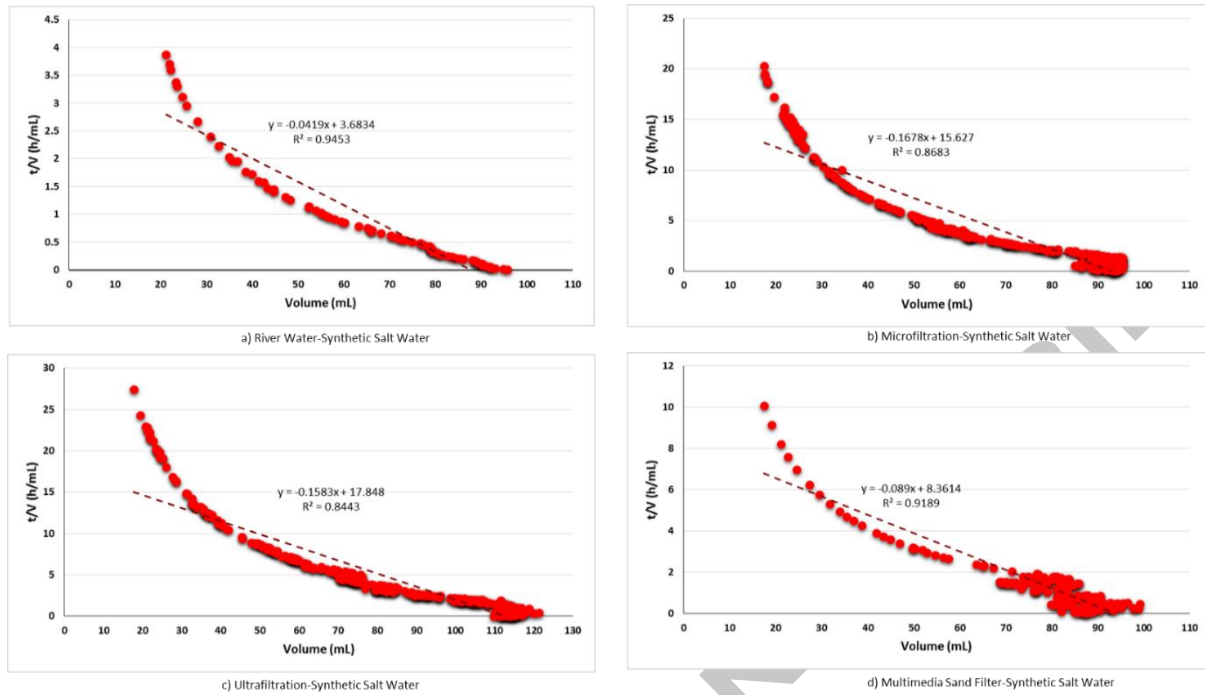


Figure 6: CFM Using Synthetic Salt Water for a) River Water, b) Microfiltration, c) Ultrafiltration, and d) Multimedia Sand Filter

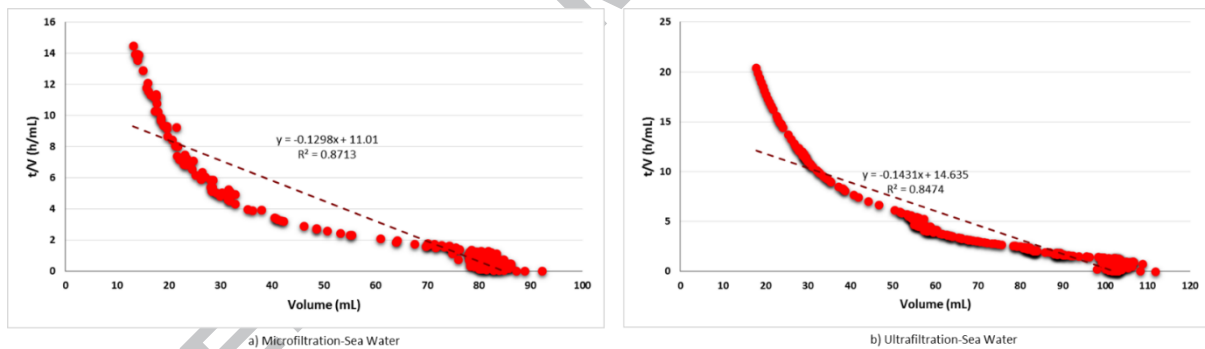


Figure 7: CFM Using Sea Water for a) Microfiltration, and b) Ultrafiltration.

Table 6: Comparison between R^2 values for each model.

Type of Feed Water	R^2 Value			
	CFM	CBM	SBM	IBM
River Water-Synthetic Salt Water	0.9453	0.7969	0.6493	0.5932
Multimedia Sand Filter-Synthetic Salt Water	0.9189	0.7795	0.6138	0.5583
Microfiltration-Synthetic Salt Water	0.8683	0.7536	0.5226	0.4510
Ultrafiltration-Synthetic Salt Water	0.8443	0.7234	0.4524	0.4181

According to the results, it seems that the CFM was the main fouling mechanism for all different feed waters (Table 6). The value of R-squared followed the order of: river water (0.95) > multimedia sand filter (0.92) > microfiltration-synthetic salt water (0.87) > ultrafiltration-synthetic salt water (0.84). These results are in accordance with the demonstrated results in section 3.1. It was interesting that the R^2 values for ultrafiltration using both draw solutions were almost the same. The same results were observed for microfiltration using sea and synthetic salt waters. According to the results in section 3.1, fouling occurred faster for ultrafiltration and microfiltration when sea water was used as the draw solution. Therefore, it can be concluded that this classic mechanism was not completely able to elaborate and explain this different behavior for osmotically driven membranes when different draw solutions were used. The reason of this phenomena will be discussed in section 3.2.4.

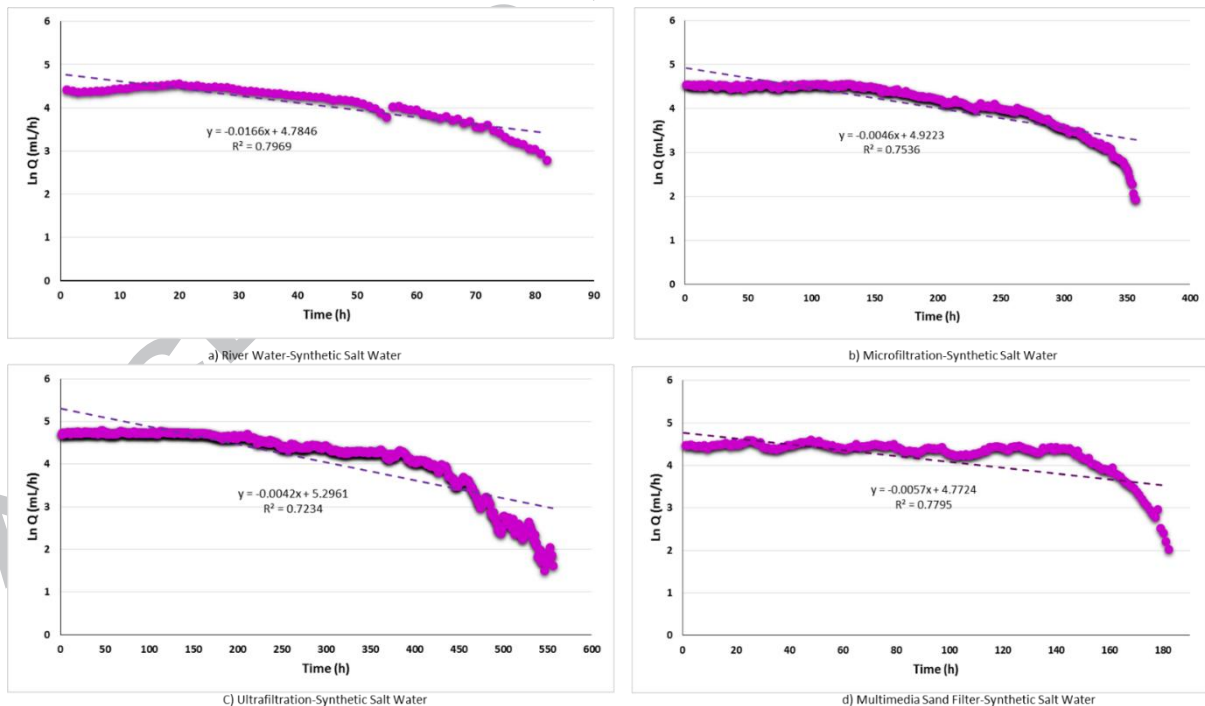


Figure 8: CBM Using Synthetic Salt Water for a) River Water, b) Microfiltration, c) Ultrafiltration, and d) Multimedia Sand Filter.

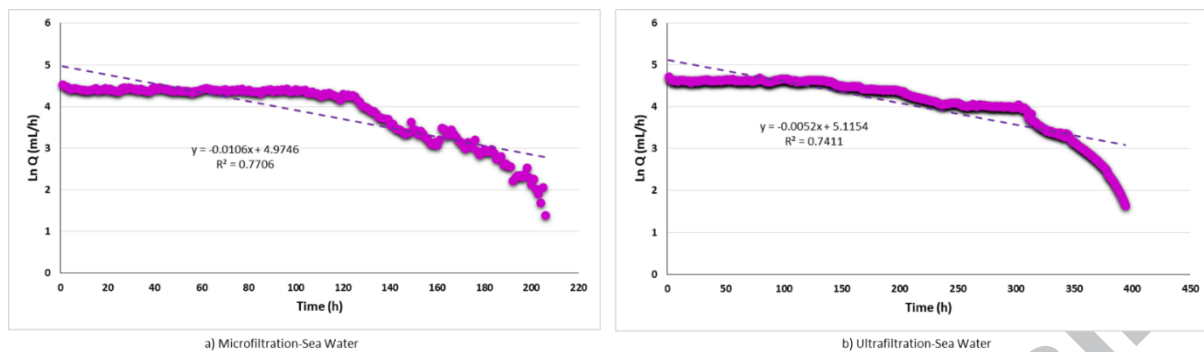


Figure 9: CBM Using Sea Water for a) Microfiltration, and b) Ultrafiltration.

In CBM, particles block the pores and prevent flow [23-25, 66]. Pore blocking is a fast process in comparison with cake formation [67]. The linearized equation that was used to study the CF model is shown in Table 5. Figures 8 and 9 show the natural logarithm of permeate flow rate versus the time for both synthetic salt and sea waters. According to the results, it can be observed that the experimental data were relatively in agreement with the CBM (Table 6). The maximum and minimum values of R-squared were 0.80 and 0.72 for river water-synthetic salt water and ultrafiltration-synthetic salt water respectively. According to the results, the value of R-squared followed the order of: river water > multimedia sand filter > microfiltration-sea water > microfiltration-synthetic salt water > ultrafiltration-sea water > ultrafiltration-synthetic salt water. These results are in accordance with the demonstrated results in section 3.1.

In IBM, it is supposed that part of the particles block the pores and the remainder are gathered on top of other deposited particles [24, 25, 66]. SBM is based on the accumulation of the particles within the membrane pores on the wall of cylindrical pores. When the deposition of the particles starts, the pores become narrower and consequently, the permeability of the membrane is decreased [23-25].

The IBM (Table 5) was applied to the obtained experimental data in section 3.1 in order to determine if the IBM was in agreement with the experimental data. According to the results shown in Table 6, the experimental data from ultrafiltration, microfiltration, multimedia sand filter and river water using synthetic salt and sea waters are not in agreement with IBM. The maximum and minimum R-squared values were 0.59 and 0.42 for river water-synthetic salt water and ultrafiltration-synthetic salt water respectively. These values are much lower than the R-squared values in CFM. The results indicated in Table 6 prove that the feasibility of this mechanism is not very high.

Table 6 demonstrates that the experimental data were not in the agreement with the SBM as well. The maximum and minimum R-squared values were 0.65 and 0.45 for river water-synthetic salt water and ultrafiltration-synthetic salt water respectively. It should be mentioned that the R-squared values in SBM were lower than the CFM. Therefore, based on the indicated results in Table 6, SBM cannot be considered as one of the main fouling mechanisms to explain the decrease of permeate flux in this research.

3.2.1 Cake Enhanced Osmotic Pressure Mechanism (CEOPM)

As it was mentioned above, the cake filtration fouling model (CFM) was not able to explain why the R-squared values were the same for ultrafiltration-synthetic salt water and ultrafiltration-sea water while the results in section 3.1.2 showed that fouling rate was not the same for them and it occurred faster for ultrafiltration-sea water compared to ultrafiltration-synthetic salt water. The same trend was also observed for microfiltration-synthetic salt water and microfiltration-sea water. A mechanism for salt rejecting membranes has been introduced which is called cake enhanced osmotic pressure (CEOP) [68-71]. In this mechanism, the back diffusion

of salt is prevented by a cake layer and as a result, the osmotic pressure increases close to the membrane surface. In osmotically driven membranes such as FO and PRO, solutes can penetrate through the membrane from the high concentration draw solution to the feed solution. This causes a considerable decline in the permeate flux and driving force in these membranes (FO and PRO) [4, 28, 61, 72]. In this experiment, the cation concentrations of sodium, calcium, magnesium and potassium were measured in sea water and synthetic salt water in order to investigate the effect of these cations on the membrane fouling in PRO mode. The concentrations of sodium and calcium in synthetic salt water were lower than that in sea water. In addition, there are magnesium and potassium in sea water which do not exist in synthetic salt water. She et al. [27] observed that sodium had the largest reverse solute diffusion rate compared to calcium and magnesium. However, it had a lower fouling rate in comparison with calcium and magnesium. In this study, although the concentration of sodium is higher in the sea water (8750 mg/L) compared to synthetic salt water (8158 mg/L), it cannot have a significant effect on the fouling rate when the draw solution was from sea water. Moreover, although sodium cation has a smaller size compared to potassium cation, its permeability through the membrane from draw solution to feed solution is lower than that of potassium cation (potassium cation is less hydrated compared to sodium cation). Therefore the reverse diffusion of potassium should be easier than sodium [73].

On the other hand, the concentration of calcium in sea water (324 mg/L) is not considerably higher than in synthetic salt water (313.77 mg/L), so its effect on fouling rate when sea water was used as the draw solution was not very significant. Therefore, magnesium and potassium had a meaningful influence in governing the fouling rate and that is why the fouling occurred faster for both ultrafiltration and

microfiltration when the used draw solution was sea water compared to when it was synthetic salt water. In order to reach the electro-neutrality of solution, more cations have to penetrate across the membrane [73]. As the concentrations of magnesium and potassium were higher in sea water, subsequently their concentration increased in the feed solution to sustain the electro-neutrality. The reverse diffusion of magnesium and potassium could alter the feed solution chemistry and consequently, enhance the membrane fouling on the feed side. Further investigation is required to model this effect in order to understand the role of reverse diffusion of draw solutes in fouling enhancement.

4 Conclusions

In this research, the fouling behavior and mechanisms of a commercial FO membrane in PRO mode by using four different feed waters (river water, multimedia sand filter, microfiltration, and ultrafiltration) and two different draw solutions (synthetic salt water and sea water) were investigated and compared. The fouling rate when the draw solution was synthetic salt water followed the order of: untreated river water > multimedia sand filter > microfiltration > ultrafiltration. The fouling rate in ultrafiltration and microfiltration using sea water occurred faster compared to the results for synthetic salt water. The cake filtration (CFM) was the main fouling mechanism for all different feed waters. According to the results, cake filtration model was not completely able to predict the observed difference in the behavior of osmotically driven membranes when different draw solutions were used. Using cake enhanced osmotic pressure mechanism, assisted to understand the effect of various draw solutions on the membrane fouling in PRO mode. As these four classic models are able to predict only one mechanism for the whole filtration process, further

investigations (considering their combination with the CEOP mechanism) are required for development of these models which will lead to a better understanding and prediction of the fouling behavior in the osmotically driven membranes.

5 Acknowledgements

The authors acknowledge the support of Mitacs, Hydro-Québec, H2O Innovation and Concordia University for this research. The authors would also like to thank Mr. Pascal Champagne, Mr. Guy. Lavallée and Mr. Yancee Bourassa for their help in the Hydro-Québec lab, as well as Mr. Erik Desormeaux from Porifera.

References

- [1] Xu, Y., X. Peng, C.Y. Tang, Q.S. Fu and S. Nie, *Effect of draw solution concentration and operating conditions on forward osmosis and pressure retarded osmosis performance in a spiral wound module*. Journal of Membrane Science, 2010. **348**: p. 298–309.
- [2] Kim, Y.C. and M. Elimelech, *Potential of osmotic power generation by pressure retarded osmosis using seawater as feed solution: Analysis and experiments*. Journal of Membrane Science, 2013. **429**: p. 330–337.
- [3] Kim, Y.C., Y. Kim, D. Oh and K.H. Lee, *Experimental Investigation of a Spiral-Wound Pressure-Retarded Osmosis Membrane Module for Osmotic Power Generation*. Environmental and Science Technology, 2013. **47**: p. 2966–2973.
- [4] She, Q., X. Jin and C.Y. Tang, *Osmotic power production from salinity gradient resource by pressure retarded osmosis: Effects of operating conditions and reverse solute diffusion*. Journal of Membrane Science, 2012. **401-402**: p. 262–273.
- [5] Álvarez-Silva, O., A. Osorio, S. Ortega and P. Agudelo-Restrepo, *Estimation of the Electric Power Potential Using Pressure Retarded Osmosis in the Leon River's Mouth: A First Step for the Harnessing of Saline Gradients in Colombia*. IEEE 2011: p. 7 pages.

- [6] Post, J.W., J. Veerman, H.V.M. Hamelers, G.J.W. Euverink, S.J. Metz, K. Nymeijer and C.J.N. Buisman, *Salinity-gradient power: Evaluation of pressure-retarded osmosis and reverse electrodialysis*. Journal of Membrane Science, 2007. **288**: p. 218–230.
- [7] Lee, J., Y. Kim, S. Shim, B. Im and W. Kim, *Numerical study of a hybrid multi-stage vacuum membrane distillation and pressure-retarded osmosis system*. Desalination, 2015. **363**: p. 82–91.
- [8] Thelin, W.R., E. Sivertsen, T. Holt and G. Brekke, *Natural organic matter fouling in pressure retarded osmosis*. Journal of Membrane Science 2013. **438**: p. 46–56.
- [9] Kim, Y.C., J.H. Lee and S. Park, *Novel cross flow membrane cell with asymmetric channels: Design and pressure-retarded osmosis performance test*. Journal of Membrane Science, 2015. **476**: p. 76–86.
- [10] Abbasi-Garravand, E., C.M. Mulligan, C.B. Laflamme and G. Clairet, *Using Ultrafiltration and Sand Filters as Two Pretreatment Methods for Improvement of the Osmotic Power (Salinity Gradient Energy) Generation Process*, in *4th Climate Change Technology Conference*. 2015: Montreal, Canada. p. 12 pages.
- [11] She, Q., Y.K.W. Wong, S. Zhao and C.Y. Tang, *Organic fouling in pressure retarded osmosis: experiments, mechanisms and implications*. Journal of Membrane Science, 2013. **428**: p. 181-189.
- [12] Kim, J., S.J. Kim and D.K. Kim, *Energy harvesting from salinity gradient by reverse electrodialysis with anodic alumina nanopores*. Energy Sources, 2013. **51**: p. 413-421.
- [13] Jiang, T., M.D. Kennedy, B.F. Guinzbourg, P.A. Vanrolleghem and J.C. Schippers, *Optimising the operation of a MBR pilot plant by quantitative analysis of the membrane fouling mechanism*. Water Science & Technology, 2005. **51**(6-7): p. 19-25.
- [14] Nghiem, L.D. and S. Hawkes, *Effects of membrane fouling on the nanofiltration of pharmaceutically active compounds (PhACs): Mechanisms and role of membrane pore size*. Separation and Purification Technology, 2007. **57**: p. 176–184.

- [15] Mi, B. and M. Elimelech, *Organic fouling of forward osmosis membranes: Fouling reversibility and cleaning without chemical reagents*. Journal of Membrane Science, 2010. **348**: p. 337–345.
- [16] Brião, V.B. and C.R.G. Tavares, *Pore blocking mechanisms for the recovery of milk solids from dairy wastewater by ultrafiltration*. Brazilian Journal of Chemical Engineering, 2012. **29**: p. 393 - 407.
- [17] Jarusutthirak, C., *Fouling and flux decline of reverse osmosis (RO), nanofiltration (NF), and ultrafiltration (UF) membranes associated with effluent organic matter (EFOM) during wastewater reclamation/reuse*, in *Department of Civil, Environmental, and Architectural Engineering*. 2002, University of Colorado. p. 322.
- [18] Mattaraj, S., C. Jarusutthirak, C. Charoensuk and R. Jiratananon, *A combined pore blockage, osmotic pressure, and cake filtration model for crossflow nanofiltration of natural organic matter and inorganic salts*. Desalination 2011. **274**: p. 182–191.
- [19] Kim, K.J., A.G. Fanea, C.J.D. Fell and D.C. Joy, *Fouling mechanisms of membranes during protein ultrafiltration*. Journal of Membrane Science, 1992. **68**: p. 79-91.
- [20] Hermans, P.H. and H.L. Bredée, *Zur kenntnis der filtrationsgesetze*. Rec. Trav. Chim. Pays-Bas, 1935. **54**(9): p. 680-700. doi: 10.1002/recl.19350540902.
- [21] Londono, I.C., *Assesment of causes of irreversible fouling in powdered activated carbon/ultrafiltration membrane (PAC/UF) systems*, in *Civil Engineering*. 2011, The University of British Columbia: Vancouver.
- [22] Hermia, J., *Constant pressure blocking filtration laws—application to power-law non-Newtonian fluids*. Transactions of the Institution of Chemical Engineers, 1982. **60**(3): p. 183–187.
- [23] Rezaei, H., F. Zokaei Ashtiani and A. Fouladitajar, *Effects of operating parameters on fouling mechanism and membrane flux in cross-flow microfiltration of whey*. Desalination, 2011. **274**: p. 262–271.
- [24] Bolton, G.R., A.W. Boesch and M.J. Lazzara, *The effects of flow rate on membrane capacity: Development and application of adsorptive membrane fouling models*. Journal of Membrane Science 2006. **279**: p. 625–634.

- [25] Bolton, G., D. LaCasse and R. Kuriyel, *Combined models of membrane fouling: Development and application to microfiltration and ultrafiltration of biological fluids*. Journal of Membrane Science 2006. **277**: p. 75–84.
- [26] Lee, S., C. Boo, M. Elimelech and S. Hong, *Comparison of fouling behavior in forward osmosis (FO) and reverse osmosis (RO)*. Journal of Membrane Science, 2010. **365**: p. 34–39.
- [27] She, Q., X. Jin, Q. Li and C.Y. Tang, *Relating reverse and forward solute diffusion to membrane fouling in osmotically driven membrane processes*. Water Research, 2012. **46**(2478-2486).
- [28] Hancock, N.T. and T.Y. Cath, *Solute coupled diffusion in osmotically driven membrane processes*. Environmental and Science Technology, 2009. **43**: p. 6769-6775.
- [29] Park, M., J. Lee, C. Boo, S. Hong, S.A. Snyder and J.H. Kim, *Modeling of colloidal fouling in forward osmosis membrane: Effects of reverse draw solution permeation*. Desalination 2013. **314**: p. 115–123.
- [30] Chen, S.C., C.F. Wan and T. Chung, *Enhanced fouling by inorganic and organic foulants on pressure retarded osmosis (PRO) hollow fiber membranes under high pressures*. Journal of Membrane Science, 2015. **479**: p. 190–203.
- [31] Reis, R.V. and A. Zydney, *Bioprocess membrane technology*. Journal of Membrane Science 2007. **297**(1-2): p. 16-50.
- [32] Daniel, R.C., J.M. Billing, R.L. Russell, R.W. Shimskey, H.D. Smith and R.A. Peterson, *Integrated pore blockage – cake filtration model for crossflow filtration*. Chemical Engineering Research and Design, 2011. **89**: p. 1094–1103.
- [33] Keskinler, B., E. Yildiz, E. Erhan, M. Dogru, Y.K. Bayhan and G. Akay, *Crossflow microfiltration of low concentration-nonliving yeast suspensions*. Journal of Membrane Science, 2004. **233**: p. 59–69.
- [34] Vera, M.C.V., S.Á. Blanco, J.L. García and E.B. Rodríguez, *Analysis of membrane pore blocking models adapted to crossflow ultrafiltration in the ultrafiltration of PEG*. Chemical Engineering Journal, 2009. **149**: p. 232–241.
- [35] Murase, T. and T. Ohn, *New decline pattern of filtrate flux in crossflow microfiltration of dilute suspension*. AIChE Journal, 1996. **42**: p. 1938–1944.

- [36] Prádanos, P., A. Hernández, J.I. Calvo and F. Tejerina, *Mechanisms of protein fouling in cross-flow UF through an asymmetric inorganic membrane*. Journal of Membrane Science, 1996. **114**: p. 115–126.
- [37] Jonsson, G., P. Prádanos and A. Hernández, *Fouling phenomena in microporous membranes: Flux decline kinetics and structural modification*. Journal of Membrane Science, 1996. **112**: p. 171–183.
- [38] Millero, F.J. and H.L. Wing, *The thermodynamics of sea water at one atmosphere*. American Journal of Science, 1976. **276**: p. 1035-1077.
- [39] Culkin, F. and R.A. Cox, *Sodium, potassium, magnesium, calcium and strontium in sea water*. Deep-Sea Research, 1966. **13**: p. 789-804.
- [40] Laflamme, C.B., *Énergie osmotique-Éléments de conception pour les bancs d'essais LTE. Rapport LTE-RT-2013-0036*. Institut de recherche d'Hydro-Québec. 2013: p. 31.
- [41] ASTM Standard D4189-07, *Standard test method for silt density index (SDI) of water*. D19.08 on membranes and ion exchange materials,, 2007.
- [42] Wei, C., S. Laborie, R.B. Aim and G. Amy, *Full utilization of silt density index (SDI) measurement for seawater pretreatment*. Journal of Membrane Science, 2012. **405-406**: p. 212-218.
- [43] Hach Company, *Methods for the examination of water, and waste water*. 2007.
- [44] Abbasi-Garravand, E., C.N. Mulligan, C.B. Laflamme and G. Clairet, *Role of two different pretreatment methods in osmotic power (salinity gradient energy) generation*. Renewable Energy, 2016. **96**: p. 98-119.
- [45] Mosqueda-Jimenez, D.B. and P.M. Huck, *Characterization of membrane foulants in drinking water treatment*. Desalination, 2006. **198**: p. 173-182.
- [46] Ødegaard, H., S. Østerhus, E. Melin and B. Eikebrokk, *NOM removal technologies – Norwegian experiences*. Drinking Water Engineering and Science, 2010. **3**: p. 1-9.
- [47] Machenbach, I. and H. Odegaard, *Relevance of Flocculation in Integrated Membrane Processes for NOM Removal*, in *in Chemical and Waste Water*

Treatment VIII: Proceeding of the 11th Gothenburg Symposium. 2004: IWA Publishing, London. p. 245-253.

- [48] Machenbach, I., T. Leiknes and H. Ødegaard, *Coagulation/submerged hollow-fibre ultrafiltration for natural organic matter removal*. *Water Science and Technology: Water Supply*, 2003. **3 (5-6)**: p. 401–407.
- [49] Abbasi-Garravand, E., C.M. Mulligan, C.B. Laflamme and G. Clairet, *Identification of the type of foulants and investigation of the membrane cleaning methods for PRO processes in osmotic power application*. *Desalination Journal*, 2017. DOI: **10.1016/j.desal.2017.01.038**.
- [50] Porifera Inc., *Specification Sheet: FOMEM-0513 July*. 2014: p. 1.
- [51] Porifera Inc., *High rejection, high flux forward osmosis membranes. FOMEM-0513 FAQ*. 2014: p. 1-2.
- [52] Hydro-Québec, *Matériel et équipement des bancs d'essai*. 2013: p. 1-5.
- [53] Li, X. and T.S. Chung, *Thin-film composite p84 co-polyimide hollow fiber membranes for osmotic power generation*. *Applied Energy*, 2014. **114**: p. 600-610.
- [54] Bui, N. and J.R. McCutcheon, *Nanofiber Supported Thin-Film Composite Membrane for Pressure- Retarded Osmosis*. *Environmental and Science Technology*, 2014. **48**: p. 4129–4136.
- [55] Chou, S., R. Wang, N. Anthony and G. Fane, *Robust and High performance hollow fiber membranes for energy harvesting from salinity gradients by pressure retarded osmosis*. *Journal of Membrane Science*, 2013. **448**: p. 44–54.
- [56] Han, G., S. Zhang, X. Li and T. Chung, *High performance thin film composite pressure retarded osmosis (PRO) membranes for renewable salinity-gradient energy generation*. *Journal of Membrane Science*, 2013. **440**: p. 108–121.
- [57] Hoover, L.A., J.D. Schiffman and M. Elimelech, *Nanofibers in thin-film composite membrane support layers: Enabling expanded application of forward and pressure retarded osmosis*. *Desalination*, 2013. **308**: p. 73–81.

- [58] Kim, H., J.S. Choi and S. Lee, *Pressure retarded osmosis for energy production: membrane materials and operating conditions*. *Water Science & Technology*, 2012. **65.10**: p. 1789-1794.
- [59] Saito, K., M. Irie, S. Zaitso, H. Sakai, H. Hayashi and A. Tanioka, *Power generation with salinity gradient by pressure retarded osmosis using concentrated brine from SWRO system and treated sewage as pure water*. *Desalination and Water Treatment*, 2012. **41**: p. 114–121.
- [60] Achilli, A., T.Y. Cath and A.E. Childress, *Power generation with pressure retarded osmosis: An experimental and theoretical investigation*. *Journal of Membrane Science*, 2009. **343**: p. 42–52.
- [61] Tang, C.Y., Q. She, W.C.L. Lay, R. Wang and A.G. Fane, *Coupled effects of internal concentration polarization and fouling on flux behavior of forward osmosis membranes during humic acid filtration*. *Journal of Membrane Science*, 2010. **354**: p. 123–133.
- [62] Chen, Y., L. Setiawan, S. Chou, X. Hu and R. Wang, *Identification of safe and stable operation conditions for pressure retarded osmosis with high performance hollow fiber membrane*. *Journal of Membrane Science* 2016. **503**: p. 90–100.
- [63] Kim, J., M.J. Park, M. Park, H.K. Shon, S. Kim and J.H. Kim, *Influence of colloidal fouling on pressure retarded osmosis*. *Desalination*, 2016. **389**: p. 207–214.
- [64] Kim, D.I., J. Kim and S. Hong, *Changing membrane orientation in pressure retarded osmosis for sustainable power generation with low fouling*. *Desalination*, 2016. **389**: p. 197–206.
- [65] Kimura, K., S. Okazaki, T. Ohashi and Y. Watanabe, *Importance of the co-presence of silica and organic matter in membrane fouling for RO filtering MBR effluent*. *Journal of Membrane Science*, 2016. **501**: p. 60–67.
- [66] Katsoufidou, K., S.G. Yiantsios and A.J. Karabelas, *A study of ultrafiltration membrane fouling by humic acids and flux recovery by backwashing: Experiments and modeling*. *Journal of Membrane Science* 2005. **266**: p. 40–50.
- [67] Song, L., *Flux decline in crossflow microfiltration and ultrafiltration: mechanisms and modeling of membrane fouling*. *Journal of Membrane Science*, 1998. **139**: p. 183-200.

- [68] Hoek, E.M.V., A.S. Kim and M. Elimelech, *Influence of crossflow membrane filter geometry and shear rate on colloidal fouling in reverse osmosis and nanofiltration separations*. Environmental and Science Technology, 2002. **19**: p. 357–372.
- [69] Herzberg, M. and M. Elimelech, *Biofouling of reverse osmosis membranes: role of biofilm-enhanced osmotic pressure*. Journal of Membrane Science, 2007. **295**: p. 11–20.
- [70] Hoek, E.M.V. and M. Elimelech, *Cake-enhanced concentration polarization: a new fouling mechanism for salt-rejecting membranes*. Environmental and Science Technology, 2003. **37**: p. 5581–5588.
- [71] Lee, S., J. Cho and M. Elimelech, *Influence of colloidal fouling and feed water recovery on salt rejection of RO and NF membranes*. Desalination 2004. **160**: p. 1–12.
- [72] Phillip, W.A., J.S. Yong and M. Elimelech, *Reverse draw solute permeation in forward osmosis: modeling and experiments*. Environmental Science and Technology, 2010. **44**: p. 5170–5176.
- [73] Heo, J., K.H. Chu, N. Her, J. Im, Y. Park, J. Cho, S. Sarp, A. Jang, M. Jang and Y. Yoon, *Organic fouling and reverse solute selectivity in forward osmosis: Role of working temperature and inorganic draw solutions*. Desalination, 2015: p. 1-9.

Figure Captions

Figure 1: a) PRO Membrane setup at Hydro-Québec Research Institute, b) schematic of PRO membrane setup.

Figure 2: Osmotic Cell Dimensions

Figure 3: Effect of Fouling on Permeate Flux using Different Feed Waters

Figure 4: Effect of Fouling on Permeate Flux Using Microfiltration as Feed Water and Sea Water and Synthetic Salt Water as Draw water.

Figure 5: Effect of Fouling on Permeate Flux Using Ultrafiltration as Feed Water and Sea Water and Synthetic Salt Water as Draw water.

Figure 6: CFM Using Synthetic Salt Water for a) River Water, b) Microfiltration, c) Ultrafiltration, and d) Multimedia Sand Filter.

Figure 7: CFM Using Sea Water for a) Microfiltration, and b) Ultrafiltration.

Figure 8: CBM Using Synthetic Salt Water for a) River Water, b) Microfiltration, c) Ultrafiltration, and d) Multimedia Sand Filter.

Figure 9: CBM Using Sea Water for a) Microfiltration, and b) Ultrafiltration.

Research highlights

- Fouling rate in ultrafiltration and microfiltration effluents using sea water was faster
- CF and cake enhanced osmotic pressure models could describe membrane fouling
- Complete fouling occurred in ultrafiltration after 580 hours
- Fouling rate order using synthetic salt water was: river water > sand filter > MF > UF

ACCEPTED MANUSCRIPT